Spin-1 quantum walks

Daichi Morita,[1] Toshihiro Kubo,[1] Yasuhiro Tokura,[1,2,*] and Makoto Yamashita[1,2]
[1]*Graduate School of Pure and Applied Sciences, University of Tsukuba, 1-1-1 Tennodai, Tsukuba, Ibaraki 305-8571, Japan*
[2]*NTT Basic Research Laboratories, NTT Corporation, 3-1 Morinosato Wakamiya, Atsugi, Kanagawa 243-0198, Japan*
(Received 18 April 2016; published 20 June 2016)

We study the quantum walks of two interacting spin-1 bosons. We derive an exact solution for the time-dependent wave function, which describes the two-particle dynamics governed by the one-dimensional spin-1 Bose-Hubbard model. We show that propagation dynamics in real space and mixing dynamics in spin space are correlated via the spin-dependent interaction in this system. The spin-mixing dynamics has two characteristic frequencies in the limit of large spin-dependent interactions. One of the characteristic frequencies is determined by the energy difference between two bound states, and the other frequency relates to the cotunneling process of a pair of spin-1 bosons. Furthermore, we numerically analyze the growth of the spin correlations in quantum walks. We find that long-range spin correlations emerge showing a clear dependence on the sign of the spin-dependent interaction and the initial state.

DOI: 10.1103/PhysRevA.93.063625

I. INTRODUCTION

Classical random walks play an important role in randomized algorithms that have been developed to achieve superior performance when solving various hard problems in computer science [1]. It is thus quite natural that quantum walks (QWs) [2–5], which are the quantum mechanical counterparts of classical random walks, become a powerful tool for building quantum algorithms, providing versatile applications such as quantum search algorithms [6,7] and universal quantum computation [8–10]. Two theoretical QW models have already been proposed: the discrete-time QW [11,12] and the continuous-time QW [13]. In discrete-time QWs, the dynamics of a walker is determined by flipping the coin state via a unitary operator at each discrete step. On the other hand, in continuous-time QWs, a walker evolves continuously on the basis of the Schrödinger equation without flipping any coin states. These two models have revealed the unique features of QWs. A walker generates a coherent superposition state as a result of multiple interferences and propagates ballistically, showing a bimodal profile of the probability distribution, which is in sharp contrast to classical random walks.

Implementations of QWs have been reported in a series of experiments using magnetic resonance, trapped ions, trapped neutral atoms, and some photonic systems [14]. In particular, in recent years, continuous-time QWs including two walkers (i.e., two indistiguishable particles) have been attracting considerable attention [15–18]. Experiments with an array of coupled nanophotonic waveguides showed that nontrivial correlations emerge in the QW dynamics of two identical photons as a consequence of Hanbury-Brown–Twiss interference [16]. In Ref. [17], Lahini *et al.* precisely analyzed how such correlations are modified in the presence of interactions between the walkers. Using the Bose-Hubbard (BH) model as a basis, they revealed that the dynamical evolution of two walkers changes greatly depending on both the interaction strengths and the initial state. This study sheds light on another important role of QWs, as a fundamental building block of quantum simulators for many-body dynamics [19,20].

Quite recently, the continuous-time QWs of two interacting particles were demonstrated using bosonic ultracold atoms in a one-dimensional (1D) optical lattice [18]. In this experiment, the high controllability of interatomic interactions is a great advantage when we investigate the dependence of particle correlations on the interaction strengths. Furthermore, the advanced technique provided by a quantum gas microscope [21,22] allows us to access directly the dynamics of QWs by resolving each atom over lattice sites [18,23]. The measured data quantitatively agree with theoretical calculations based on the BH model. These features convince us that ultracold atoms can offer a promising platform on which we develop quantum simulations via multiparticle QWs.

We further expect that ultracold atoms will advance the study of QWs to the unexplored region where walkers contain internal degrees of freedom. The atom manipulation technique currently provides us with the multicomponent many-body system referred to as a spinor Bose gas [24–29]. It is known that this system exhibits diverse and complex quantum phases caused by the interplay between interactions and spin degrees of freedom [30–40]. In particular, the spin-1 bosonic atom system has been intensively studied as the simplest spinor Bose gas. The spin-dependent interaction of spin-1 atoms generates transitions among the spin states that preserve the z component of the total spin [41]. This phenomenon is called spin-mixing dynamics and has been observed using a spin-1 Bose-Einstein condensate in a single optical trap [42–44] and also in an optical lattice [45–48]. Therefore, the QWs of spin-1 bosons present an intriguing problem, namely, clarification of the dynamical evolution of walkers that are interfering and interacting and mixing of spins under conditions where the total energy and total spins are both conserved.

In this paper, we study a continuous-time QW including two spin-1 bosons trapped in a 1D optical lattice. We focus mainly on spin-mixing dynamics, which is one of the most intriguing features of spin-1 systems. Furthermore, spin correlations as well as spatial correlations [17] can be studied with this model. Exploring the evolution of spin correlations helps further our understanding of the dynamics involving spins in spin-1 lattice systems.

This paper is organized as follows. In Sec. II, we introduce the spin-1 BH model and explain the spin-mixing dynamics in

*tokura.yasuhiro.ft@u.tsukuba.ac.jp

a single-site system. In Sec. III, we derive the exact solution of the two-particle dynamics governed by the spin-1 BH model. Using the results in Sec. III, we discuss the spin-mixing dynamics in quantum walks in Sec. IV. The dependence on the interaction strength is discussed in detail. In Sec. V, we explain how the spin-dependent interaction affects the evolution of spin correlations. Finally, we conclude the text in Sec. VI. In the Appendix, we derive the spin-mixing dynamics in an alternative way based on the effective Hamiltonian.

II. MODEL

We consider spin-1 bosons in a 1D optical lattice. These atoms are well described by the spin-1 BH Hamiltonian,

$$\hat{H} = \hat{H}_J + \hat{H}_{U_0} + \hat{H}_{U_2}, \tag{1}$$

$$\hat{H}_J = -J \sum_{i,\alpha=0,\pm1} (\hat{b}^\dagger_{i+1,\alpha}\hat{b}_{i,\alpha} + \text{H.c.}), \tag{2}$$

$$\hat{H}_{U_0} = \frac{U_0}{2}\sum_i \hat{n}_i(\hat{n}_i - 1), \tag{3}$$

$$\hat{H}_{U_2} = \frac{U_2}{2}\sum_i \left(\hat{\mathbf{F}}_i^2 - 2\hat{n}_i\right), \tag{4}$$

where $\hat{b}^\dagger_{i,\alpha}$ ($\hat{b}_{i,\alpha}$) is the bosonic creation (annihilation) operator at the ith site with the hyperfine spin state $\alpha(=0,\pm1)$, and $\hat{n}_i = \sum_{\alpha=0,\pm1}\hat{b}^\dagger_{i,\alpha}\hat{b}_{i,\alpha}$ is the corresponding local number operator. $\hat{\mathbf{F}}_i$ denotes the hyperfine spin operator at the ith site defined in terms of 3×3 spin-1 matrices $F^{x,y,z}$ as $\hat{F}^x_i = \sum_{\alpha,\beta}\hat{b}^\dagger_{i,\alpha}(F^x)_{\alpha,\beta}\hat{b}_{i,\beta}$, etc. $\hat{H}_J$, $\hat{H}_{U_0}$, and $\hat{H}_{U_2}$ represent the nearest-neighbor hopping, spin-independent interactions, and spin-dependent interactions, respectively. $\hat{H}_{U_2}$ induces a transition among states, which preserves the z component of the total spin $\sum_i \hat{F}^z_i$. The spin dependence of the interactions arises from the difference between the scattering lengths for the total spins $F = 0$ and $F = 2$. To obtain an exact analysis, we restrict the discussion to a two-particle system. Furthermore, we set $\hbar$ and the lattice constant at unity throughout this paper.

It is useful in relation to our later discussions of quantum walks that we briefly explain the dynamics of two interacting spin-1 bosons localized at a certain single site with only $\hat{H}_{U_0}$ and $\hat{H}_{U_2}$ (i.e., $J = 0$). In the absence of an external magnetic field, we can discuss the intriguing spin-mixing dynamics without loss of generality in a limited case where the quantum state of spin-1 bosons is given by the superposition of two spin states with the same z component of the total spin, i.e., $m_F = 0$. Such states are $|F=0,m_F=0\rangle = ((\hat{b}^\dagger_0)^2 - 2\hat{b}^\dagger_1\hat{b}^\dagger_{-1})|0\rangle/\sqrt{6}$ and $|F=2,m_F=0\rangle = ((\hat{b}^\dagger_0)^2 + \hat{b}^\dagger_1\hat{b}^\dagger_{-1})|0\rangle/\sqrt{3}$, and the corresponding eigenenergies are $E_{F=0} = -2U_2$ and $E_{F=2} = U_2$, respectively [49,50]. The time evolution of the quantum mechanical average of an operator $\hat{O}$ is evaluated via state $|\psi(t)\rangle$ at time t:

$$\begin{aligned}\langle\hat{O}\rangle_t &= \langle\psi(t)|\hat{O}|\psi(t)\rangle,\\ &= \sum_{F,F'} e^{i(E_F-E_{F'})t}\sum_{m_F,m'_F}[\langle F,m_F|\hat{O}|F',m'_F\rangle\\ &\quad\times\langle\psi(0)|F,m_F\rangle\langle F',m'_F|\psi(0)\rangle].\end{aligned} \tag{5}$$

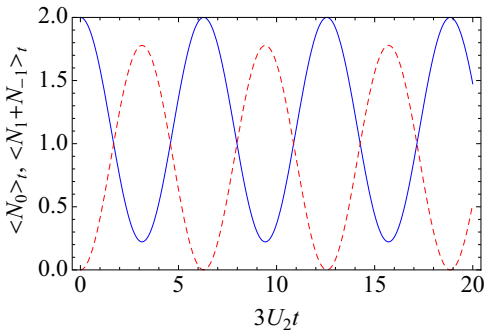

FIG. 1. Spin-mixing dynamics in the single-site system ($J = 0$). Solid and dashed lines represent the populations as a function of time in the spin state $\alpha = 0$ and the sum of the populations in spin states $\alpha = \pm1$, respectively.

Let us consider a case where two atoms stay in the hyperfine spin state of $\alpha = 0$ at the initial time $t = 0$: $|\psi(0)\rangle = (\hat{b}^\dagger_0)^2/\sqrt{2}|0\rangle = \sqrt{1/3}|F=0,m_F=0\rangle + \sqrt{2/3}\,|F=2,m_F=0\rangle$. Using Eq. (5), we obtain the average number of atoms in the hyperfine spin state $\alpha = 0,\pm1$ at time t:

$$\langle\hat{N}_0\rangle_t = \frac{10 + 8\cos(3U_2t)}{9}, \tag{6}$$

$$\langle\hat{N}_1\rangle_t = \frac{4 - 4\cos(3U_2t)}{9} = \langle\hat{N}_{-1}\rangle_t. \tag{7}$$

Figure 1 shows the time evolution of the spin-state populations calculated from Eqs. (6) and (7). The spin-mixing dynamics emerges owing to the $\hat{H}_{U_2}$ term in the Hamiltonian. The oscillation frequency $3U_2(=E_{F=2} - E_{F=0})$ corresponds to the energy difference between the two states that we consider here.

In the following sections, we show how such regular spin-mixing dynamics is modified by the intersite hopping processes ($J \neq 0$).

III. EXACT SOLUTION

In this section, we analyze the quantum dynamics of two spin-1 bosons based on the Hamiltonian in Eq. (1). We derive the time-dependent wave function exactly by employing the method developed by Deuchert *et al.* in Ref. [51].

The hopping of spin-1 atoms does not change their internal spin states; i.e., the two states $|F=0,m_F=0\rangle$ and $|F=2,m_F=0\rangle$ are not connected to each other via the hopping process. This allows us to straightforwardly generalize the bases $|F,m_F\rangle$ in the single-site system to the bases in the lattice system:

$$|\psi_{-2U_2}\rangle_{i,j} = \frac{1}{\sqrt{6}}[\hat{b}^\dagger_{i,0}\hat{b}^\dagger_{j,0} - \hat{b}^\dagger_{i,1}\hat{b}^\dagger_{j,-1} - \hat{b}^\dagger_{i,-1}\hat{b}^\dagger_{j,1}]|0\rangle, \tag{8}$$

$$|\psi_{U_2}\rangle_{i,j} = \frac{1}{\sqrt{3}}\left[\hat{b}^\dagger_{i,0}\hat{b}^\dagger_{j,0} + \frac{\hat{b}^\dagger_{i,1}\hat{b}^\dagger_{j,-1} + \hat{b}^\dagger_{i,-1}\hat{b}^\dagger_{j,1}}{2}\right]|0\rangle. \tag{9}$$

Here the orthonormality is satisfied such that ${}_{i,j}\langle\psi_\lambda|\psi_{\lambda'}\rangle_{k,\ell} = \delta_{\lambda,\lambda'}(\delta_{i,k}\delta_{j,\ell} + \delta_{i,\ell}\delta_{j,k})/2$, where λ and λ' take $-2U_2$ or U_2. These bases also span all the eigenstates of the Hamiltonian in Eq. (1). Furthermore, in each spanned space represented by the quantum number $\lambda = -2U_2$ or U_2, the Hamiltonian

becomes equivalent to the spinless BH Hamiltonian $\hat{H}_J + \hat{H}_{U_0}$ by replacing U_0 with $U_0 - 2U_2$ for Eq. (8) and with $U_0 + U_2$ for Eq. (9). This means that the dynamics of two interacting spin-1 bosons is essentially identical to that of spinless bosons, which greatly simplifies the theoretical treatment. Since the two-particle dynamics governed by the spinless BH model is exactly solvable by introducing center-of-mass coordinates $R = (i + j)/2$ and relative coordinates $r = i - j$ [51], we can calculate the exact dynamics for the spin-1 BH model. The eigenenergies and eigenstates in each space specified by λ consist of scattering states and bound states. Hence the Schrödinger equations are written as

$$\hat{H}\left|\Psi^B_{\lambda,K}\right\rangle = E^B_{\lambda,K}\left|\Psi^B_{\lambda,K}\right\rangle,$$
$$\hat{H}\left|\Psi^S_{\lambda,K,k}\right\rangle = E^S_{K,k}\left|\Psi^S_{\lambda,K,k}\right\rangle, \tag{10}$$

where K and k represent the center-of-mass and the relative quasimomenta, respectively. We obtain the eigenenergies and eigenstates

$$E^B_{\lambda,K} = \mathrm{sgn}(U_0+\lambda)\sqrt{(U_0+\lambda)^2 + 16J^2[\cos(K/2)]^2}, \tag{11}$$

$$\left|\psi^B_{\lambda,K}\right\rangle = {\sum_{R,r}}' \frac{1}{\sqrt{2\pi}} e^{iKR} \frac{\sqrt{|\mathcal{U}_{\lambda,K}|}}{\left(\mathcal{U}^2_{\lambda,K}+1\right)^{1/4}} \times \left[\mathcal{U}_{\lambda,K} - \mathrm{sgn}(U_0+\lambda)\sqrt{\mathcal{U}^2_{\lambda,K}+1}\right]^{|r|} \times |\psi_\lambda\rangle_{R+r/2,R-r/2} \tag{12}$$

for bound states and

$$E^S_{K,k} = -4J\cos(K/2)\cos(k), \tag{13}$$

$$\left|\psi^S_{\lambda,K,k}\right\rangle = {\sum_{R,r}}' \frac{\frac{1}{\sqrt{2\pi}}e^{iKR}}{\sqrt{\pi\left(1+\frac{\mathcal{U}^2_{\lambda,K}}{\sin^2(k)}\right)}} \times \left[\cos(kr) + \frac{\mathcal{U}_{\lambda,K}}{\sin(k)}\sin(k|r|)\right]|\psi_\lambda\rangle_{R+r/2,R-r/2} \tag{14}$$

for scattering states. Here we employ the abbreviations $J_K = 2J\cos(K/2)$, $\mathcal{U}_{\lambda,K} = (U_0+\lambda)/2J_K$, and ${\sum_{R,r}}' = \sum_{R\in\mathbf{Z}}\sum_{r\in 2\mathbf{Z}} + \sum_{R\in\mathbf{Z}+1/2}\sum_{r\in 2\mathbf{Z}+1}$. Note that the energies of the scattering states are independent of interactions. Figure 2 illustrates the energy spectra as a function of the center-of-mass quasimomentum K. The band of bound states is split into two depending on the spin-dependent interaction U_2 and located above the continuum of scattering states when $U_0/J > 0$ and $U_0 > 2U_2$. If we take $U_2/U_0 = 1/2$ or -1, one of the bands disappears.

Eigenstates satisfy the following orthonormality relations:

$$\left\langle\psi^B_{\lambda',K'}\middle|\psi^B_{\lambda,K}\right\rangle = \delta_{\lambda,\lambda'}\delta(K-K'), \tag{15}$$

$$\left\langle\psi^S_{\lambda',K',k'}\middle|\psi^S_{\lambda,K,k}\right\rangle = \delta_{\lambda,\lambda'}\delta(K-K')\delta(k-k'), \tag{16}$$

$$\left\langle\psi^S_{\lambda',K',k'}\middle|\psi^B_{\lambda,K}\right\rangle = 0. \tag{17}$$

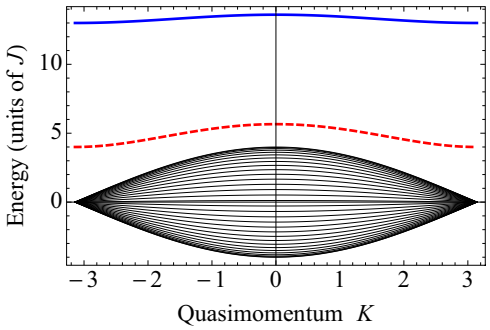

FIG. 2. Energy spectra for $U_2/U_0 = 0.3$ and $U_0/J = 10$ as a function of the center-of-mass quasimomentum K. Thick solid and dashed lines correspond to the energy bands for bound states with $F = 2$ and $F = 0$, respectively. The bundle of thin solid lines represents the scattering continuum. The energy is defined in units of J.

Now the initial state at time $t = 0$ is generally written as a superposition of eigenstates Eqs. (8) and (9),

$$|\Psi(0)\rangle = \sum_\lambda \int_{-\pi}^{\pi} dK \left[a_{\lambda,K}\left|\psi^B_{\lambda,K}\right\rangle + \int_0^\pi dk\, b_{\lambda,K,k}\left|\psi^S_{\lambda,K,k}\right\rangle\right], \tag{18}$$

where the coefficients $a_{\lambda,K}$ and $b_{\lambda,K,k}$ satisfy the proper normalization condition

$$\langle\Psi(0)|\Psi(0)\rangle = \sum_\lambda \int_{-\pi}^{\pi} dK \left[|a_{\lambda,K}|^2 + \int_0^\pi dk |b_{\lambda,K,k}|^2\right] = 1. \tag{19}$$

When two atoms are initially located at the same site, the normalized number of atoms in the bound states of the subspace λ [first term of Eq. (19)] becomes

$$N_{B,\lambda} = \int_{-\pi}^{\pi} dK\, |a_{\lambda,K}|^2 = c_\lambda \frac{2}{\pi}\frac{U_0+\lambda}{E^B_{\lambda,0}} G\left(\frac{16J^2}{{E^B_{\lambda,0}}^2}\right). \tag{20}$$

Here, $G(m) = \int_0^{\pi/2} \frac{1}{\sqrt{1-m\sin^2\theta}} d\theta$ represents the complete elliptic function of the first kind and c_λ is the normalized number of atoms in the subspace λ, which is determined by the choice

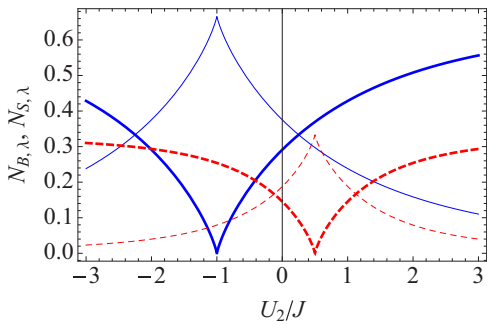

FIG. 3. Normalized number of bound states and scattering states in each space spanned by Eqs. (8) and (9) as a function of the spin-dependent interaction. Thick and thin lines represent the normalized number of atoms in bound states and scattering states, respectively. Solid and dashed lines correspond to the indices $\lambda = U_2$ and $\lambda = -2U_2$, respectively. We assume a condition where two $\alpha = 0$ atoms occupy the same site and we choose $U_0/J = 1$.

of the initial state. If we start from two $\alpha = 0$ atoms at the same site, $c_{U_2} = 2/3$ and $c_{-2U_2} = 1/3$. Figure 3 shows the normalized number of bound states and scattering states in each space with respect to the spin-dependent interaction. Because of Eq. (19), the normalized number of atoms in the scattering states of the subspace λ becomes $N_{S,\lambda} = c_\lambda - N_{B,\lambda}$. Clearly, the normalized number of atoms in the bound states, Eq. (20), increases with the absolute value of the interaction in each space. This is natural because the bound states are created by the interaction.

By definition, the state at time t is straightforwardly given by

$$\begin{aligned}|\Psi(t)\rangle &= \sum_\lambda \int_{-\pi}^{\pi} dK \Big[a_{\lambda,K} e^{iE^B_{\lambda,K}t} \big|\psi^B_{\lambda,K}\big\rangle \\ &\quad + \int_0^\pi dk b_{\lambda,K,k} e^{iE^S_{K,k}t} \big|\psi^S_{\lambda,K,k}\big\rangle \Big] \\ &\equiv \sum_{i,j}\sum_\lambda \Psi_\lambda(i,j,t)|\psi_\lambda\rangle_{i,j}. \end{aligned} \tag{21}$$

This result enables us to calculate any physical quantities of the two-particle dynamics governed by the spin-1 BH model.

IV. SPIN-MIXING DYNAMICS IN QUANTUM WALKS

In this section, we discuss the spin-mixing dynamics in QWs. We show in detail that the intersite hopping of atoms in the lattice system greatly changes the simple oscillation behavior of spin-mixing dynamics discussed in Sec. II.

A. Analytical results

The spin-mixing dynamics is described by the total number of atoms in a hyperfine state α. The quantum mechanical average at time t ($\langle\cdot\rangle_t = \langle\Psi(t)|\cdot|\Psi(t)\rangle$) of the corresponding operator $\hat{N}_\alpha = \sum_i \hat{b}^\dagger_{i,\alpha}\hat{b}_{i,\alpha}$ is calculated to be

$$\begin{aligned}\langle\hat{N}_0\rangle_t &= \frac{2}{3}\sum_{i,j}\Big(\big|\Psi_{-2U_2}(i,j,t)\big|^2 + 2\big|\Psi_{U_2}(i,j,t)\big|^2 \\ &\quad + 2\sqrt{2}\mathrm{Re}\big[\Psi^*_{-2U_2}(i,j,t)\Psi_{U_2}(i,j,t)\big]\Big), \end{aligned} \tag{22}$$

$$\begin{aligned}\langle\hat{N}_1\rangle_t &= \frac{1}{3}\sum_{i,j}\Big(2\big|\Psi_{-2U_2}(i,j,t)\big|^2 + \big|\Psi_{U_2}(i,j,t)\big|^2 \\ &\quad - 2\sqrt{2}\mathrm{Re}\big[\Psi^*_{-2U_2}(i,j,t)\Psi_{U_2}(i,j,t)\big]\Big) = \langle\hat{N}_{-1}\rangle_t. \end{aligned} \tag{23}$$

The function defined in Eq. (21) can be expressed using the initial state $|\psi(0)\rangle$

$$\Psi_\lambda(i,j,t) \equiv \sum_{i',j'} {}_{i',j'}\langle\psi_\lambda|\Psi(0)\rangle W^\lambda_{i,j;i',j'}(t), \tag{24}$$

where

$$\begin{aligned}&W^\lambda_{R,r;R',r'}(t) \\ &\quad = \int_{-\pi}^{\pi}\frac{dK}{2\pi}e^{iK(R-R')}\big[w^B_{\lambda,K}(r,r',t) + w^S_{\lambda,K}(r,r',t)\big], \end{aligned} \tag{25}$$

is a matrix element of the time evolution operator in the space λ. Here, we introduce $R' = (i'+j')/2$ and $r' = i' - j'$. $w^B_{\lambda,K}(r,r',t)$ and $w^S_{\lambda,K}(r,r',t)$ correspond to the contributions of bound states and scattering states, respectively. The explicit formulas of these functions are

$$\begin{aligned}w^B_{\lambda,K}(r,r',t) &= \frac{|\mathcal{U}_{\lambda,K}|}{\sqrt{1+\mathcal{U}^2_{\lambda,K}}}e^{-iE^B_{\lambda,K}t} \\ &\quad \times\Big[\mathcal{U}_{\lambda,K} - \mathrm{sgn}(U_0+\lambda)\sqrt{\mathcal{U}^2_{\lambda,K}+1}\Big]^{|r|+|r'|}, \end{aligned} \tag{26}$$

$$w^S_{\lambda,K}(r,r',t) = \int_0^\pi \frac{dk}{\pi}e^{-iE^S_{K,k}t}\frac{f_{\lambda,K}(r)f_{\lambda,K}(r')}{1+\frac{\mathcal{U}^2_{\lambda,K}}{\sin^2(k)}}, \tag{27}$$

with

$$f_{\lambda,K}(n) = \cos(kn) + \frac{\mathcal{U}_{\lambda,K}}{\sin(k)}\sin(k|n|). \tag{28}$$

When two atoms in the hyperfine state $\alpha = 0$ are initially located at the origin of a 1D lattice, the projection of this initial state onto each space is given by

$${}_{i',j'}\big\langle\psi_{U_2}\big|\Psi(0)\big\rangle = \sqrt{\frac{2}{3}}\delta_{i',0}\delta_{j',0}, \tag{29}$$

$${}_{i',j'}\big\langle\psi_{-2U_2}\big|\Psi(0)\big\rangle = \frac{1}{\sqrt{3}}\delta_{i',0}\delta_{j',0}. \tag{30}$$

Hence the total number of $\alpha = 0$ atoms at time t becomes

$$\begin{aligned}\langle\hat{N}_0\rangle_t &= \frac{1}{9}\left(10 + 8{\sum_{R,r}}'\mathrm{Re}\big[W^{-2U_2}_{R,r;0,0}{}^*(t)W^{U_2}_{R,r;0,0}(t)\big]\right) \\ &\equiv \frac{1}{9}[10 + 8(X_B(t) + X_S + X_{BS}(t))]. \end{aligned} \tag{31}$$

From Eq. (25), the matrix element W is the sum of the contributions of the bound states [Eq. (26)] and scattering states [Eq. (27)]. We can thus separate the time-dependent term of $\langle\hat{N}_0\rangle_t$ into three parts: the product of the contribution of the bound states, X_B, the product of the contribution of the scattering states, X_S, and the interference between the contributions of the bound and scattering states, X_{BS}. Specifically,

$$X_B(t) = \frac{(U_0-2U_2)(U_0+U_2)}{2U_0-U_2}\int_{-\pi}^{\pi}\frac{dK}{2\pi}\frac{E^B_{-2U_2,K}+E^B_{U_2,K}}{E^B_{-2U_2,K}E^B_{U_2,K}}\cos\big[\big(E^B_{-2U_2,K}-E^B_{U_2,K}\big)t\big], \tag{32}$$

$$X_S = 1 - \frac{2}{\pi}\frac{1}{2U_0-U_2}\left[\frac{(U_0+U_2)^2}{E^B_{U_2,0}}G\left(\frac{16J^2}{{E^B_{U_2,0}}^2}\right) + \frac{(U_0-2U_2)^2}{E^B_{-2U_2,0}}G\left(\frac{16J^2}{{E^B_{-2U_2,0}}^2}\right)\right], \tag{33}$$

$$X_{BS}(t) = 3U_2\int_{-\pi}^{\pi}\frac{dK}{2\pi}\int_0^\pi\frac{dk}{\pi}\left[\frac{A_{K,k}(U_0-2U_2)}{1+\frac{\mathcal{U}^2_{U_2,K}}{\sin^2(k)}} - \frac{A_{K,k}(U_0+U_2)}{1+\frac{\mathcal{U}^2_{-2U_2,K}}{\sin^2(k)}}\right], \tag{34}$$

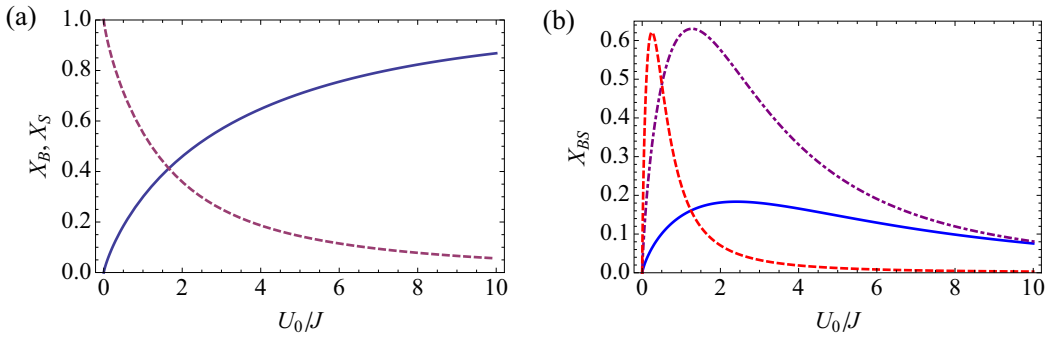

FIG. 4. Interaction dependence of X_B, X_S, and X_{BS} at $t = 0$. (a) $U_2/U_0 = 0.3$. Solid and dashed lines represent X_B and X_S, respectively. (b) Interference term $X_{BS}(0)$ for three U_2/U_0 values. Solid, dot-dashed, and dashed lines correspond to $U_2/U_0 = 0.3$, 1, and 5, respectively.

with

$$A_{K,k}(\lambda) = \frac{U_0+\lambda}{E^B_{\lambda,K}} \frac{\left(U_0+\lambda-E^B_{\lambda,K}\right)\cos\left[\left(E^B_{\lambda,K}-E^S_{K,k}\right)t\right]}{16J^2[\cos(K/2)]^2+\left(U_0+\lambda+E^S_{K,k}\right)\left(U_0+\lambda-E^B_{\lambda,K}\right)}. \tag{35}$$

Here the function $G(m)$ represents the complete elliptic integral of the first kind. The time-independent nature of X_S comes from the interaction independence of the energy of the scattering states. X_S is calculated via the product of $w^*_{-2U_2,K}$ and $w_{U_2,K}$, and its time dependence is determined by the difference between the energies in the exponential part included in the $w_{\lambda,K}$ function. However, $E^S_{K,k}$ in Eq. (13) clearly shows that this energy difference vanishes and therefore X_S becomes independent of time. Regarding X_B and X_{BS}, it is difficult to derive their expressions as a function of time t by analytically dealing with the integrals with respect to quasimomenta in Eqs. (32) and (34). Instead, at $t = 0$, we can perform the integrals and obtain the following useful expressions:

$$X_B(0) = \frac{2}{\pi}\frac{(U_0+U_2)(U_0-2U_2)}{2U_0-U_2} \times\left[\frac{1}{E^B_{U_2,0}}G\left(\frac{16J^2}{{E^B_{U_2,0}}^2}\right)+\frac{1}{E^B_{-2U_2,0}}G\left(\frac{16J^2}{{E^B_{-2U_2,0}}^2}\right)\right], \tag{36}$$

$$X_{BS}(0) = -\frac{2}{\pi}\frac{3U_2}{2U_0-U_2}\left[\frac{U_0-2U_2}{E^B_{-2U_2,0}}G\left(\frac{16J^2}{{E^B_{-2U_2,0}}^2}\right) - \frac{U_0+U_2}{E^B_{U_2,0}}G\left(\frac{16J^2}{{E^B_{U_2,0}}^2}\right)\right]. \tag{37}$$

Then we can immediately find $X_B(0)+X_S+X_{BS}(0) = 1$, which is consistent with the choice of the initial condition. A similar calculation shows

$$\langle\hat{N}_1\rangle_t = \tfrac{1}{9}[4-4(X_B(t)+X_S+X_{BS}(t))] = \langle\hat{N}_{-1}\rangle_t. \tag{38}$$

We note that Eq. (31) [Eq. (38)] has the same form as Eq. (6) [Eq. (7)] because the constant term comes from the norm of the wave functions in each space, which does not change with time.

B. Numerical results

We carried out numerical calculations to reveal the properties of the spin-mixing dynamics in a lattice system. Although the ratio U_2/U_0 is rather low in experiments such as ^{23}Na (positive) and ^{87}Rb (negative), i.e., less than a few percent, here we choose $U_2/U_0 = 0.3$ to demonstrate the effect of spin-dependent interactions more clearly. Figure 4 shows X_B, X_S, and X_{BS} at the initial time $t = 0$ as a function of the normalized interaction strength U_0/J. In Fig. 4(a), the contribution of the bound states $X_B(0)$ gradually increases with the interaction, while the contribution of the scattering states X_S decreases with the interaction. This reflects the fact that the interaction reduces the number of particles in the scattering states [see Eq. (14)]. Since the energy of the initially localized state must be conserved, the interaction suppresses the dissociation of the pair [52]. On the other hand, the interference term $X_{BS}(0)$ exhibits a nonmonotonic dependence on the interaction, reaching a maximum at around $U_0/J \sim 1$ [see Fig. 4(b)]. However, $X_{BS}(t)$ rapidly decreases with time as shown in Fig. 5. This characteristic time dependence can be interpreted by considering the evolution of the bound and scattering states. The wave functions of the scattering states spread over the lattice with time, while the wave functions of the bound states remain localized. The overlaps between these two kinds of states decrease with time. Hence we neglect X_{BS} in the following discussion.

Next we analyze the spin-mixing dynamics based on Eqs. (31) and (38). Figure 6 shows the time evolution of the total number of atoms in the hyperfine state α corresponding to four U_2/J values. We see that the spin-mixing dynamics is highly sensitive to the interactions. For a large U_2/J, there are two distinct frequencies and the amplitude of the slower oscillation gradually decreases with time. We elucidate the dependence of the two frequencies on the interactions from the results of a spectral analysis: the higher frequency ω_{high} coincides with the characteristic frequency of spin mixing in the single-site system $3U_2$ and the lower frequency ω_{low} is reduced as the interaction decreases. For a low U_2/J with the fixed ratio

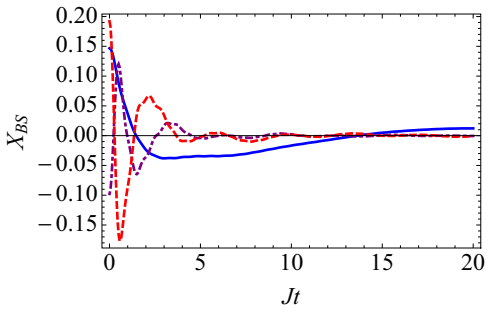

FIG. 5. Time dependence of the interference term X_{BS}. We choose three sets of interactions U_0 and U_2 in the vicinity of the maximum point of $X_{BS}(0)$ in Fig. 4(b). Solid, dot-dashed, and dashed lines correspond to $(U_0/J, U_2/U_0) = (1, 0.3)$, $(2, 1)$, and $(0.5, 5)$, respectively.

$U_2/U_0 = 0.3$, the spin-mixing dynamics is highly suppressed. This behavior stems from the fact that the coefficient of $X_B(t)$ becomes small in the vicinity of $U_0 - 2U_2 = 0$ or $U_0 + U_2 = 0$. In these situations, the number of atoms in the bound states decreases. Moreover, the reduction in the frequencies ω_{high} and ω_{low} [see Fig. 7(b)] around $U_2 = 0$ makes it difficult to observe the spin mixing. Finally, all results discussed in this section are completely applicable when the U_0 sign changes while the ratio U_2/U_0 is maintained, because of the symmetry of the dynamics governed by the 1D spinless BH model [51].

C. Discussion

Here, we reveal why two frequencies appear in the spin-mixing dynamics by taking the limits of both $U_0 + U_2 \gg 4J$ and $U_0 - 2U_2 \gg 4J$. In these limits, $X_B(t)$ becomes

$$X_B(t) \simeq \mathcal{J}_0(2\epsilon t)\cos[(3U_2 - 2\epsilon)t], \tag{39}$$

where $\mathcal{J}_n(x)$ denotes the Bessel function of the first kind. $\epsilon = J_{U_0-2U_2} - J_{U_0+U_2}$ is related to the cotunneling process, namely, the simultaneous hopping of two particles at the same site to an adjacent site. $J_U \equiv 2J^2/U$ is the effective hopping of the cotunneling process in the large interaction limit, $U/J \gg 1$ [53]. Using the addition theorem of the Bessel function, $\mathcal{J}_m(x-y) = \sum_{n=-\infty}^{\infty} \mathcal{J}_n(x)\mathcal{J}_{n-m}(y)$, with $|x| > |y|$, the factor $\mathcal{J}_0(2\epsilon t)$ can be rewritten as

$$\begin{aligned}\mathcal{J}_0(2\epsilon t) &= \sum_n \mathcal{J}_n\left(2J_{U_0-2U_2}t\right)\mathcal{J}_n\left(2J_{U_0+U_2}t\right), \\ &= \sum_n \psi^*_{J_{U_0-2U_2}}(n,t)\psi_{J_{U_0+U_2}}(n,t).\end{aligned} \tag{40}$$

Here, $\psi_J(n,t) = i^{|n|}\mathcal{J}_{|n|}(2Jt)$ is the wave function of the continuous-time QW (dynamics of a single particle initially located at the origin, governed by H_J) at the nth site at time t [54]. Hence, one can say that the Bessel function in Eq. (39) represents the overlap of the bound-state wave functions in different bands. In the limit of $U_0/J \to \infty$, ϵ becomes 0 and thus the Bessel function becomes 1. Since X_S and X_{BS} disappear in this limit, Eq. (31) [Eq. (38)] coincides with Eq. (6) [Eq. (7)]. Note that Eq. (39) can also be derived by using the effective Hamiltonian for bound states (see the Appendix).

Since Eq. (39) is the product of periodic and quasiperiodic functions, the frequencies of the spin-mixing dynamics are determined by the sum and the difference between the frequencies of each function. The sum $\omega_+ = [(3U_2 - 2\epsilon) + 2\epsilon] = 3U_2$ is identical to the frequency in a single-site system [see Eqs. (6) and (7)]. Because the approximation in Eq. (39)

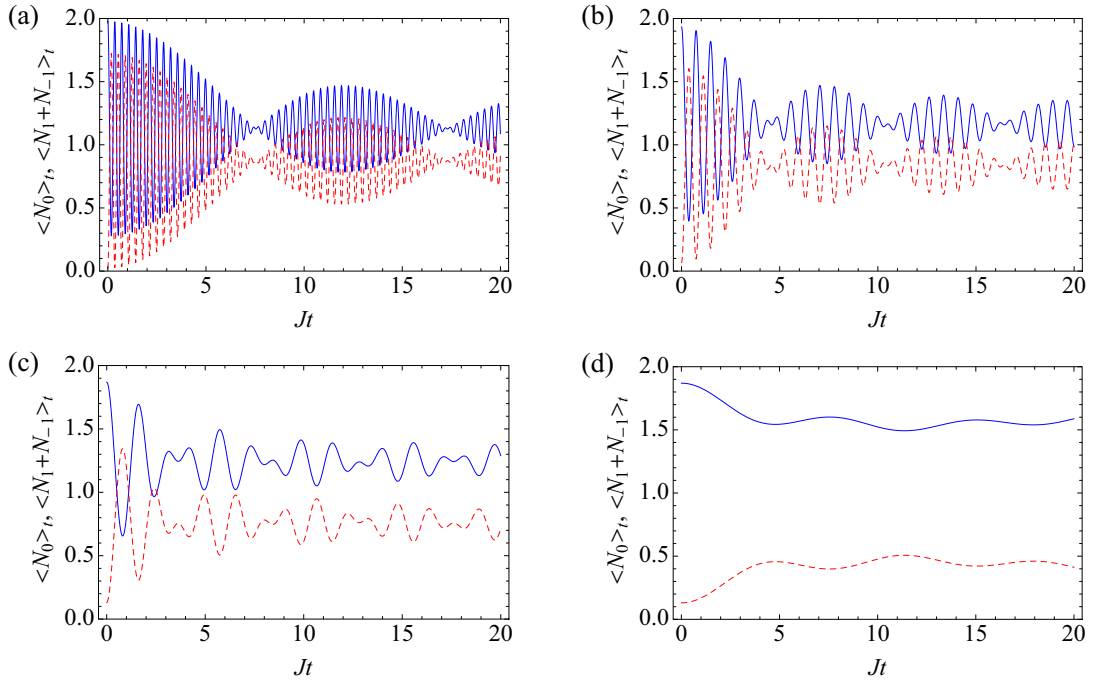

FIG. 6. Spin-mixing dynamics in a 1D optical lattice for four U_2/J values under the condition $U_2/U_0 = 0.3$: (a) $U_2/J = 6$, (b) $U_2/J = 3$, (c) $U_2/J = 1.5$, and (d) $U_2/J = 0.3$. Solid and dashed lines represent populations in spin state $\alpha = 0$ and the sum of the populations in spin states $\alpha = \pm 1$, respectively.

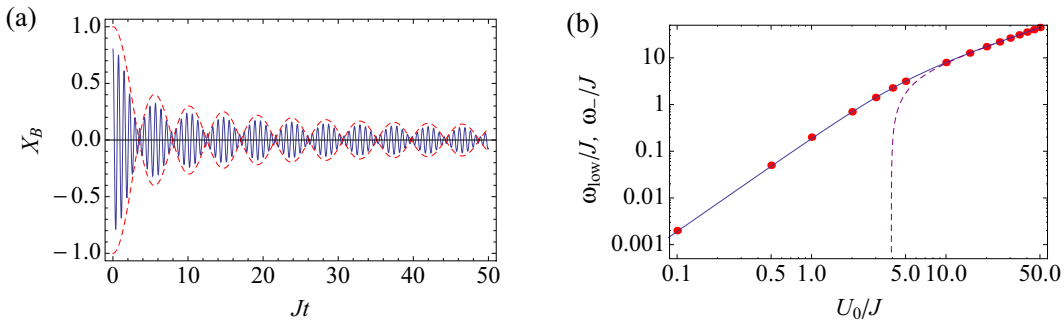

FIG. 7. (a) Time dependence of the bound-state term $X_B(t)$. Interactions are $U_0/J = 10$ and $U_2/U_0 = 0.3$. Envelope functions plotted by dashed lines correspond to $\pm\mathcal{J}_0(\epsilon' t)$. (b) Three characteristic frequencies of spin-mixing dynamics as a function of U_0: $\omega_{\rm low}$ (circle), $\omega_-(\epsilon)$ (dashed line), and $\omega_-(\epsilon')$ (solid line).

cannot be established for $U/J \sim 1$, the difference $\omega_-(\epsilon) = [(3U_2 - 2\epsilon) - 2\epsilon] = 3U_2 - 4\epsilon$ does not coincide with $\omega_{\rm low}$, which is the lower frequency calculated from the spin-mixing dynamics [see the dashed line and circles in Fig. 7(b)]. Since $4J_U$ coincides with the bandwidth of the bound states in the large-interaction limit, we consider the exact bandwidth of the bound states $4J'_U = U - \mathrm{sgn}(U)\sqrt{U^2 + 16J^2}$, instead of $4J_U$. Then ϵ becomes

$$\epsilon' = \left|J'_{U_0-2U_2} - J'_{U_0+U_2}\right|. \tag{41}$$

Substituting ϵ' for $\omega_-, \omega_-(\epsilon')$ coincides with $\omega_{\rm low}$ [see the solid line and circles in Fig. 7(b)]. As shown in Fig. 7(a), $\pm\mathcal{J}_0(2\epsilon' t)$ well describes the envelope function of $X_B(t)$. Surprisingly, ω_+ is always correct even for small interactions (compared with $\omega_{\rm high}$).

V. EMERGENCE OF LONG-RANGE SPIN CORRELATIONS

Quantum correlations in the 1D bosonic two-particle QW are discussed in Refs. [17,18] on the basis of the spinless BH model. It has been clarified that the time evolution of the two-particle correlation depends strongly on both the interaction strength and the initial condition of the QWs. When two bosons are initially localized at the same site, the relative motion is suppressed with increases in interactions. In contrast, when two bosons are initially located at adjacent sites, the relative motion is enhanced as the interaction increases. These dynamical properties can be understood by noting the energy conservation of the system. Let us consider a case where two bosons are localized at the same site. The repulsive (attractive) interaction makes the energy of this boson pair higher (lower) than the energy of the other states. The two bosons therefore tend to maintain their localized states to conserve energy [52]. For the same reason, the spatially separated bosons rarely occupy the same site, leading to the enhancement of relative motion.

In the spin-1 boson system, we observed the similar two-particle correlations mentioned above. Thus we focus on the evolution of two-particle spin correlations given by $\langle \hat{F}_{z,i}\hat{F}_{z,j}\rangle_t$. To elucidate the role of spin-dependent interaction, we choose the initial state, which does not have nonlocal spin correlations ($i \neq j$) for $U_2 = 0$. This state corresponds to the superposition of a parallel spin state and an antiparallel spin state with an equal ratio,

$$\left|\Psi^{\theta}_{i,j}(0)\right\rangle = A_{i,j}\hat{B}^{\dagger}_i(\theta)\hat{B}^{\dagger}_j(\theta)|0\rangle, \tag{42}$$

where $A_{i,j} \equiv 1/(\sqrt{4 + 2\delta_{i,j}})$ is a normalization factor and $\hat{B}^{\dagger}_j(\theta) \equiv \hat{b}^{\dagger}_{j,1} + e^{i\theta}\hat{b}^{\dagger}_{j,-1}$ is a corresponding creation operator with an arbitrary angle θ. From Eqs. (8) and (9), and also by introducing the spin states $|\uparrow\uparrow\rangle_{i,j} \equiv \hat{b}^{\dagger}_{i,1}\hat{b}^{\dagger}_{j,1}|0\rangle/\sqrt{2}$ and $|\downarrow\downarrow\rangle_{i,j} \equiv \hat{b}^{\dagger}_{i,-1}\hat{b}^{\dagger}_{j,-1}|0\rangle/\sqrt{2}$, we can rewrite the initial state in a more informative way:

$$\left|\Psi^{\theta}_{i,j}(0)\right\rangle = \sqrt{2}A_{i,j}\Bigg[|\uparrow\uparrow\rangle_{i,j} + e^{2i\theta}|\downarrow\downarrow\rangle_{i,j} + \sqrt{\frac{2}{3}}e^{i\theta}|\psi_{U_2}\rangle_{i,j} - \frac{2}{\sqrt{3}}e^{i\theta}\left|\psi_{-2U_2}\right\rangle_{i,j}\Bigg]. \tag{43}$$

Here $|\uparrow\uparrow\rangle_{i,j}, |\downarrow\downarrow\rangle_{i,j}$ and $|\psi_{U_2}\rangle_{i,j}$ correspond to the three basis states of the total spin $F = 2$ states with an interaction energy of $U_0 + U_2$, and they give the positive spin correlations. On the other hand, $|\psi_{-2U_2}\rangle_{i,j}$ is the basis of the $F = 0$ state with an interaction energy of $U_0 - 2U_2$, and it gives negative spin correlations. All these four states evolve separately over time while keeping their spin states as discussed in Sec. III. Therefore, the time dependence of two-particle spin correlations is determined by the quantum-mechanical superposition of spins during dynamical evolution in QWs. Under the condition of a finite U_2, we can expect the emergence of nonlocal spin correlations owing to the difference in interaction energy mentioned above.

Figure 8 shows simulation results for spin correlations at $t = 5/J$ calculated with $U_0/J = 2$ and $\theta = 0$. We further assume the spin-dependent interaction $U_2 = 0.3U_0$ in Figs. 8(a) and 8(c) and $U_2 = -0.3U_0$ in Figs. 8(b) and 8(d). We find that the long-range spin correlations depend strongly on the sign of U_2 and the initial states, which is a characteristic of two-particle QWs of interacting spin-1 bosons.

First, we consider a case where two spin-1 bosons are initially localized at the origin $|\Psi^0_{0,0}(0)\rangle$. Long-range spin correlations ($|i - j| \gg 1$) are negative for $U_2/U_0 > 0$ [see Fig. 8(a)] and positive for $U_2/U_0 < 0$ [see Fig. 8(b)]. We can understand this property as follows. The interaction greatly suppresses the relative motion of two spin-1 bosons for this initial state, which is similar to the spinless case. On the other hand, a spin-dependent interaction decreases the whole interaction energy and then enhances the relative motions for the $F = 0$ ($F = 2$) states when $U_2/U_0 > 0$ ($U_2/U_0 < 0$). Correspondingly, long-range spin correlations become negative (positive).

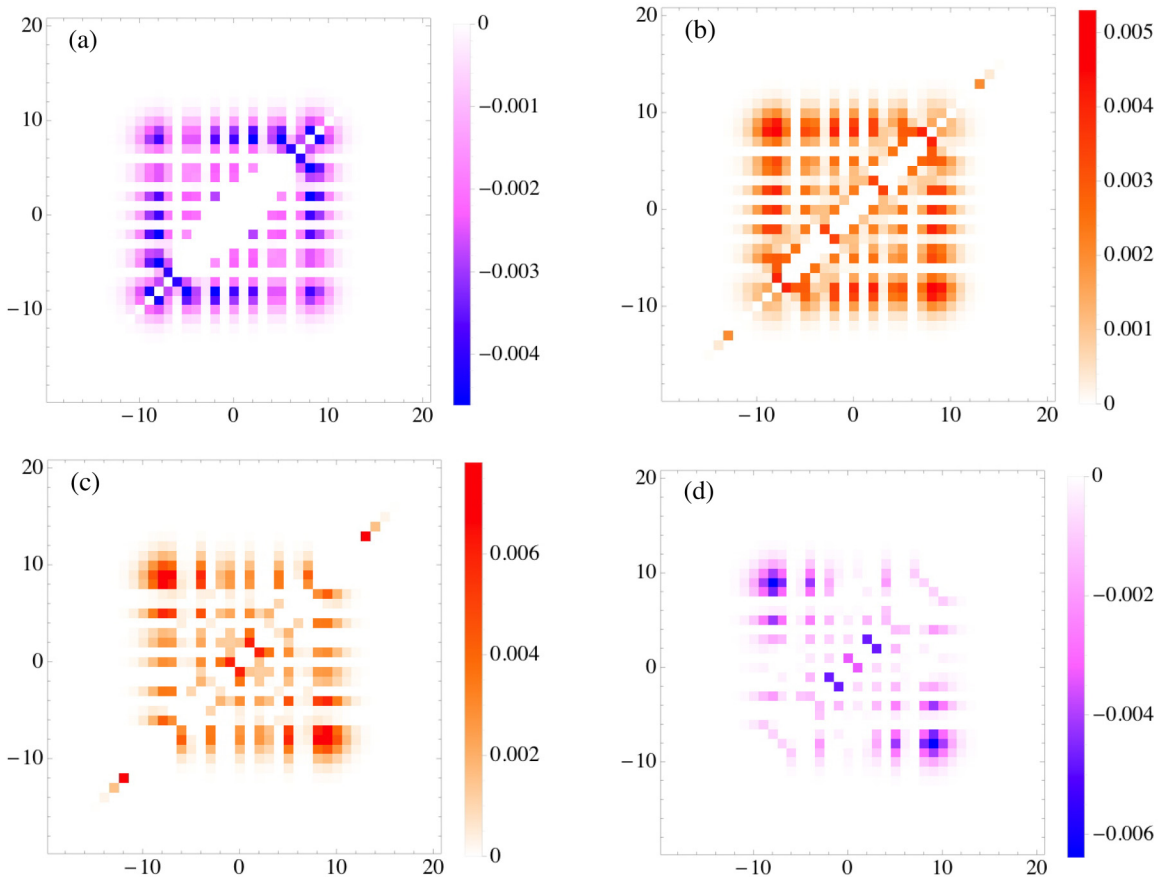

FIG. 8. Two-particle spin correlations at $t = 5/J$ calculated with $U_0/J = 2$ and $\theta = 0$. The vertical and horizontal axes represent the lattice site indices. (a), (b) Spin correlations starting from the initial state $|\Psi^0_{0,0}(0)\rangle$ where two spin-1 bosons are placed at the origin. (c), (d) Spin correlations for the initial state $|\Psi^0_{0,1}(0)\rangle$ where two bosons are placed at the origin and at the first site. We assume a positive U_2/U_0 in (a) and (c) and a negative U_2/U_0 in (b) and (d).

Next, we start from the spatially separated initial state $|\Psi^0_{0,1}(0)\rangle$, i.e., each spin-1 boson is initially located at the origin and the first site. Long-range spin correlations become positive for $U_2/U_0 > 0$ [see Fig. 8(c)] and negative for $U_2/U_0 < 0$ [see Fig. 8(d)]. For this type of initial state, the interaction enhances relative motions. By noting the spin-dependent interaction, the relative motions of $F = 2$ ($F = 0$) states are relatively enhanced for $U_2/U_0 > 0$ ($U_2/U_0 < 0$), leading to positive (negative) long-range spin correlations.

Note that two-particle spin correlations do not show any dependence on the angle θ. Therefore, we show the results for $\theta = 0$ only.

VI. CONCLUSION

In this work, we have studied the QWs of interacting spin-1 bosons on the basis of the 1D spin-1 BH model. We derive an exact expression for the time-dependent wave function by extending the method developed in Ref. [51] to a case including the spin degrees of freedom. Using this expression, the spin-mixing dynamics in QWs is discussed in detail both analytically and numerically. We show that the spin-mixing dynamics is characterized by two frequencies in the limit of large spin-dependent interaction. One of the two frequencies is determined by the energy difference between two bound states and coincides with the characteristic frequency of the spin-mixing dynamics in a single-site system. The other frequency is related to the cotunneling process, which is the simultaneous hopping of a pair of atoms between lattice sites. These properties indicate that the dynamics in the spin space is strongly correlated with the dynamical evolution in real space via spin-dependent interactions. We find that the spin-mixing amplitude is suppressed in the vicinity of interactions satisfying $U_0 - 2U_2 = 0$ or $U_0 + U_2 = 0$ because the number of spin-1 bosons in bound states is greatly reduced there.

We also numerically investigate two-particle spin correlations in the present system. Long-range spin-correlations emerge and the signs of the spin correlations can be controlled by changing the sign of the spin-dependent interaction and/or the initial condition. This owes to the fact that the spin-dependent interaction effectively shifts the spin-independent interaction in accordance with the subspace specified by the total spin $F = 0$ or $F = 2$.

Experiments with ultracold atoms have been making rapid progress in recent years. The results presented here will be demonstrated experimentally in the near-future. An interesting idea for future work is to extend the present study to a case including quadratic Zeeman effects, which are induced by magnetic fields [55] or microwaves [47], and examine how the spin-mixing dynamics is modified. Although we

focus on a system of interacting spin-1 bosons in this paper, generalization to other spinful boson systems can be realized by performing similar calculations. On the other hand, from the viewpoint of two-particle dynamics, spin mixing is a universal phenomenon in various spinful systems except for spin-1/2. It might be another intriguing problem to study spin-mixing dynamics in fermionic systems and determine the qualitative difference between bosons and fermions.

Our study paves the way for exploring continuous-time QWs including the internal degrees of freedom. This opens up the possibility of searching novel algorithmic applications of QWs by utilizing spin degrees of freedom. Furthermore, the nontrivial QW dynamics in combination with spin mixing that we elucidate in this paper will offer a clue to understanding the equilibration or thermalization processes in spinful systems.

ACKNOWLEDGMENT

This work was supported by Japan Society for the Promotion of Science KAKENHI Grant No. 25287104.

APPENDIX: THE EFFECTIVE HAMILTONIAN

Here we derive Eq. (39) in an alternative way. We introduce the following effective Hamiltonian, which describes a strongly correlated boson pair in the bound state,

$$\hat{H}^B_{\rm eff}=J_U\sum_j(\hat{R}^\dagger_j\hat{R}_{j+1}+{\rm H.c.})+(U+2J_U)\sum_j\hat{R}^\dagger_j\hat{R}_j, \quad \text{(A1)}$$

where J_U is the cotunneling amplitude, and $\hat{R}_j=(\hat{b}_j)^2/\sqrt{2}$ represents the annihilation operator of a boson pair at the jth site. Note that in deriving Eq. (A1) we should retain the constant energy shift, which explicitly depends on the interaction strength. On the basis of this Hamiltonian, we obtain the dynamical evolution of the atom pair that is initially located at the origin:

$$\Psi^B_U(R,r,t)\simeq\delta_{r,0}e^{-iUt/\hbar}e^{-2iJ_Ut}i^{-R}\mathcal{J}_R(2J_Ut). \quad \text{(A2)}$$

This is the wave function of single-particle continuous-time QWs. Then it is straightforward to derive

$$\begin{aligned}X_B(t)&=\sum_{R,r}{}'{\rm Re}\left[{\Psi^B_{U_0-2U_2}}^*(R,r,t)\Psi^B_{U_0+U_2}(R,r,t)\right]\\&\simeq\mathcal{J}_0(2\epsilon t)\cos[(3U_2-2\epsilon)t]. \quad \text{(A3)}\end{aligned}$$

[1] R. Motwani and P. Raghavan, *Randomized Algorithms* (Cambridge University Press, Cambridge, UK, 1995).

[2] A. Ambainis, Quantum walks and their algorithmic applications, Int. J. Quantum Inf. **01**, 507 (2003).

[3] J. Kempe, Quantum random walks: An introductory overview, Contemp. Phys. **44**, 307 (2003).

[4] V. Kendon, Decoherence in quantum walks—a review, Math. Struct. Comput. Sci. **17**, 1169 (2007).

[5] S. E. Venegas-Andraca, Quantum walks: A comprehensive review, Quantum Inf. Proc. **11**, 1015 (2012).

[6] N. Shenvi, J. Kempe, and K. B. Whaley, Quantum random-walk search algorithm, Phys. Rev. A **67**, 052307 (2003).

[7] A. M. Childs and J. Goldstone, Spatial search by quantum walk, Phys. Rev. A **70**, 022314 (2004).

[8] A. M. Childs, Universal Computation by Quantum Walk, Phys. Rev. Lett. **102**, 180501 (2009).

[9] N. B. Lovett, S. Cooper, M. Everitt, M. Trevers, and V. Kendon, Universal quantum computation using the discrete-time quantum walk, Phys. Rev. A **81**, 042330 (2010).

[10] A. M. Childs, D. Gosset, and Z. Webb, Universal computation by multiparticle quantum walk, Science **339**, 791 (2013).

[11] D. Aharonov, A. Ambainis, J. Kempe, and U. Vazirani, Quantum walks on graphs, in *Proceedings of the Thirty-third Annual ACM Symposium on Theory of Computing*, *STOC '01* (Association for Computing Machinery, New York, 2001), p. 50.

[12] A. Ambainis, E. Bach, A. Nayak, A. Vishwanath, and J. Watrous, One-dimensional quantum walks, in *Proceedings of the Thirty-third Annual ACM Symposium on Theory of Computing*, *STOC '01* (Association for Computing Machinery, New York, 2001), p. 37.

[13] E. Farhi and S. Gutmann, Quantum computation and decision trees, Phys. Rev. A **58**, 915 (1998).

[14] K. Manouchehri and J. Wang, *Physical Implementation of Quantum Walks* (Springer, Berlin, 2013).

[15] Y. Bromberg, Y. Lahini, R. Morandotti, and Y. Silberberg, Quantum and Classical Correlations in Waveguide Lattices, Phys. Rev. Lett. **102**, 253904 (2009).

[16] A. Peruzzo, M. Lobino, J. C. F. Matthews, N. Matsuda, A. Politi, K. Poulios, X.-Q. Zhou, Y. Lahini, N. Ismail, K. Wörhoff, Y. Bromberg, Y. Silberberg, M. G. Thompson, and J. L. O'Brien, Quantum walks of correlated photons, Science **329**, 1500 (2010).

[17] Y. Lahini, M. Verbin, S. D. Huber, Y. Bromberg, R. Pugatch, and Y. Silberberg, Quantum walk of two interacting bosons, Phys. Rev. A **86**, 011603 (2012).

[18] P. M. Preiss, R. Ma, M. E. Tai, A. Lukin, M. Rispoli, P. Zupancic, Y. Lahini, R. Islam, and M. Greiner, Strongly correlated quantum walks in optical lattices, Science **347**, 1229 (2015).

[19] I. Bloch, J. Dalibard, and S. Nascimbene, Quantum simulations with ultracold quantum gases, Nat. Phys. **8**, 267 (2012).

[20] I. M. Georgescu, S. Ashhab, and F. Nori, Quantum simulation, Rev. Mod. Phys. **86**, 153 (2014).

[21] J. F. Sherson, C. Weitenberg, M. Endres, M. Cheneau, I. Bloch, and S. Kuhr, Single-atom-resolved fluorescence imaging of an atomic Mott insulator, Nature **467**, 68 (2010).

[22] C. Weitenberg, M. Endres, J. F. Sherson, M. Cheneau, P. Schausz, T. Fukuhara, I. Bloch, and S. Kuhr, Single-spin addressing in an atomic Mott insulator, Nature **471**, 319 (2011).

[23] T. Fukuhara, P. Schausz, M. Endres, S. Hild, M. Cheneau, I. Bloch, and C. Gross, Microscopic observation of magnon bound states and their dynamics, Nature **502**, 76 (2013).

[24] D. M. Stamper-Kurn, M. R. Andrews, A. P. Chikkatur, S. Inouye, H.-J. Miesner, J. Stenger, and W. Ketterle, Optical Confinement of a Bose-Einstein Condensate, Phys. Rev. Lett. **80**, 2027 (1998).

[25] T.-L. Ho, Spinor Bose Condensates in Optical Traps, Phys. Rev. Lett. **81**, 742 (1998).
[26] T. Ohmi and K. Machida, Bose-Einstein condensation with internal degrees of freedom in alkali atom gases, J. Phys. Soc. Jpn. **67**, 1822 (1998).
[27] M. D. Barrett, J. A. Sauer, and M. S. Chapman, All-Optical Formation of an Atomic Bose-Einstein Condensate, Phys. Rev. Lett. **87**, 010404 (2001).
[28] Y. Kawaguchi and M. Ueda, Spinor Bose-Einstein condensates, Phys. Rep. **520**, 253 (2012).
[29] D. M. Stamper-Kurn and M. Ueda, Spinor Bose gases: Symmetries, magnetism, and quantum dynamics, Rev. Mod. Phys. **85**, 1191 (2013).
[30] E. Demler and F. Zhou, Spinor Bosonic Atoms in Optical Lattices: Symmetry Breaking and Fractionalization, Phys. Rev. Lett. **88**, 163001 (2002).
[31] A. Imambekov, M. Lukin, and E. Demler, Spin-exchange interactions of spin-one bosons in optical lattices: Singlet, nematic, and dimerized phases, Phys. Rev. A **68**, 063602 (2003).
[32] M. Snoek and F. Zhou, Microscopic wave functions of spin-singlet and nematic Mott states of spin-one bosons in high-dimensional bipartite lattices, Phys. Rev. B **69**, 094410 (2004).
[33] S. Tsuchiya, S. Kurihara, and T. Kimura, Superfluid-Mott insulator transition of spin-1 bosons in an optical lattice, Phys. Rev. A **70**, 043628 (2004).
[34] K. V. Krutitsky and R. Graham, Spin-1 bosons with coupled ground states in optical lattices, Phys. Rev. A **70**, 063610 (2004).
[35] T. Kimura, S. Tsuchiya, and S. Kurihara, Possibility of a First-Order Superfluid-Mott-Insulator Transition of Spinor Bosons in an Optical Lattice, Phys. Rev. Lett. **94**, 110403 (2005).
[36] M. Rizzi, D. Rossini, G. De Chiara, S. Montangero, and R. Fazio, Phase Diagram of Spin-1 Bosons on One-Dimensional Lattices, Phys. Rev. Lett. **95**, 240404 (2005).
[37] V. Apaja and O. F. Syljuåsen, Dimerized ground state in the one-dimensional spin-1 boson Hubbard model, Phys. Rev. A **74**, 035601 (2006).
[38] M. Yamashita and M. W. Jack, Spin structures of spin-1 bosonic atoms trapped in an optical lattice with harmonic confinement, Phys. Rev. A **76**, 023606 (2007).
[39] Y. Toga, H. Tsuchiura, M. Yamashita, K. Inaba, and H. Yokoyama, Mott transition and spin structures of spin-1 bosons in two-dimensional optical lattice at unit filling, J. Phys. Soc. Jpn. **81**, 063001 (2012).
[40] L. de Forges de Parny, F. Hébert, V. G. Rousseau, and G. G. Batrouni, Interacting spin-1 bosons in a two-dimensional optical lattice, Phys. Rev. B **88**, 104509 (2013).
[41] C. K. Law, H. Pu, and N. P. Bigelow, Quantum Spins Mixing in Spinor Bose-Einstein Condensates, Phys. Rev. Lett. **81**, 5257 (1998).
[42] J. Stenger, S. Inouye, D. M. Stamper-Kurn, H. J. Miesner, A. P. Chikkatur, and W. Ketterle, Spin domains in ground-state Bose-Einstein condensates, Nature **396**, 345 (1998).
[43] M.-S. Chang, Q. Qin, W. Zhang, L. You, and M. S. Chapman, Coherent spinor dynamics in a spin-1 Bose condensate, Nat. Phys. **1**, 111 (2005).
[44] J. Kronjäger, C. Becker, M. Brinkmann, R. Walser, P. Navez, K. Bongs, and K. Sengstock, Evolution of a spinor condensate: Coherent dynamics, dephasing, and revivals, Phys. Rev. A **72**, 063619 (2005).
[45] A. Widera, F. Gerbier, S. Fölling, T. Gericke, O. Mandel, and I. Bloch, Coherent Collisional Spin Dynamics in Optical Lattices, Phys. Rev. Lett. **95**, 190405 (2005).
[46] A. Widera, F. Gerbier, S. Fölling, T. Gericke, O. Mandel, and I. Bloch, Precision measurement of spin-dependent interaction strengths for spin-1 and spin-2 ^{87}Rb atoms, New J. Phys. **8**, 152 (2006).
[47] F. Gerbier, A. Widera, S. Fölling, O. Mandel, and I. Bloch, Resonant control of spin dynamics in ultracold quantum gases by microwave dressing, Phys. Rev. A **73**, 041602 (2006).
[48] L. Zhao, J. Jiang, T. Tang, M. Webb, and Y. Liu, Antiferromagnetic Spinor Condensates in a Two-Dimensional Optical Lattice, Phys. Rev. Lett. **114**, 225302 (2015).
[49] M. Koashi and M. Ueda, Exact Eigenstates and Magnetic Response of Spin-1 and Spin-2 Bose-Einstein Condensatesx, Phys. Rev. Lett. **84**, 1066 (2000).
[50] T.-L. Ho and S. K. Yip, Fragmented and Single Condensate Ground States of Spin-1 Bose Gas, Phys. Rev. Lett. **84**, 4031 (2000).
[51] A. Deuchert, K. Sakmann, A. I. Streltsov, O. E. Alon, and L. S. Cederbaum, Dynamics and symmetries of a repulsively bound atom pair in an infinite optical lattice, Phys. Rev. A **86**, 013618 (2012).
[52] K. Winkler, G. Thalhammer, F. Lang, R. Grimm, J. Hecker Denschlag, A. J. Daley, A. Kantian, H. P. Büchler, and P. Zoller, Repulsively bound atom pairs in an optical lattice, Nature **441**, 853 (2006).
[53] S. Folling, S. Trotzky, P. Cheinet, M. Feld, R. Saers, A. Widera, T. Muller, and I. Bloch, Direct observation of second-order atom tunnelling, Nature **448**, 1029 (2007).
[54] N. Konno, Limit theorem for continuous-time quantum walk on the line, Phys. Rev. E **72**, 026113 (2005).
[55] G. Breit and I. I. Rabi, Measurement of nuclear spin, Phys. Rev. **38**, 2082 (1931).